



Contents lists available at ScienceDirect

Journal of Controlled Release

journal homepage: [www.elsevier.com/locate/jconrel](http://www.elsevier.com/locate/jconrel)

## Sunlight triggered photodynamic ultradeformable liposomes against *Leishmania braziliensis* are also leishmanicidal in the dark

Jorge Montanari<sup>a</sup>, Cristina Maidana<sup>b</sup>, Mónica Inés Esteva<sup>b</sup>, Cristina Salomon<sup>c</sup>, Maria Jose Morilla<sup>a</sup>, Eder L. Romero<sup>a,\*</sup>

<sup>a</sup> Programa de Nanomedicinas, Departamento de Ciencia y Tecnología, Universidad Nacional de Quilmes, Roque Saenz Peña 352, Bernal, B1876 BXD, Buenos Aires, Argentina

<sup>b</sup> Instituto Nacional de Parasitología Dr. Mario Fatala Chaben, Paseo Colon 568, 1063, Buenos Aires, Argentina

<sup>c</sup> Área Microbiología, Facultad de Ciencias Médicas, Universidad Nacional de Cuyo. Av. Libertador 80. Centro Universitario, 5500, Mendoza. Argentina

### ARTICLE INFO

#### Article history:

Received 15 June 2010

Accepted 11 August 2010

Available online xxx

#### Keywords:

Ultradeformable liposomes

Cutaneous leishmaniasis

Photodynamic therapy

Transcutaneous

### ABSTRACT

Being independent of artificial power sources, self administered sunlight triggered photodynamic therapy 22 could be suitable alternative treatment for cutaneous leishmaniasis, that avoids the need for injectables 23 and the toxic side effects of pentavalent antimonials. In this work we have determined the *in vitro* 24 leishmanicidal activity of sunlight triggered photodynamic ultradeformable liposomes (UDL). ZnPc is a 25 hydrophobic Zn phthalocyanine that showed 20% anti-promastigote activity (APA) and 20% anti- 26 amastigote activity (AA) against *Leishmania braziliensis* (strain 2903) after 15 min sunlight irradiation 27 (15 J/cm<sup>2</sup>). However, when loaded in UDL as UDL-ZnPc (1.25 μM ZnPc–1 mM phospholipids) it elicited 28 100% APA and 80% AA at the same light dose. In the absence of host cell toxicity, UDL and UDL-ZnPc also 29 showed non-photodynamic leishmanicidal activity. Confocal laser scanning microscopy of cryosectioned 30 human skin mounted in non-occlusive Saarbrücken Penetration Model, showed that upon transcutaneous 31 administration ZnPc penetrated nearly 10 folds deeper as UDL-ZnPc that if loaded in conventional 32 liposomes. Quantitative determination of ZnPc confirmed that UDL-ZnPc penetrated homogeneously in 33 the *stratum corneum*, carrying 7 folds higher amount of ZnPc 8 folds deeper than L-ZnPc. It is envisioned 34 that the multiple leishmanicidal effects of UDL-ZnPc could play a synergistic role in prophylaxis or 35 therapeutic at the first stages of the infection. 36

© 2010 Published by Elsevier B.V. 37

### 1. Introduction

Cutaneous (CL) and mucocutaneous leishmaniasis (MCL) are 43 clinical manifestations of a group of diseases caused by dimorphic 44 protozoa that belong to different species of the *Leishmania* genus, [1] 45 which are transmitted to humans by sandfly bites. Infective parasites 46 are hosted in skin macrophages and produce ulcerative lesions [2] as 47 well as destructive mucosa inflammation in MCL [3]. 1.5 million new 48 cases of CL arise worldwide each year [4], presenting a complex 49 epidemiology that depends on intra and inter species variations [5]. The 50 CL's geographic incidence is heterogeneous, including densely affected 51 foci and dissemination areas in constant change [6] due to emigrations, 52 tourism [7,8], urbanization [9] and the expansion of suitable ecosys- 53 tems for the vector due to climatic changes [10]. A marked increase of 54 cases in Europe and America has been recorded in the last decades, and 55 new important epidemic foci have emerged [4,11].

Standard treatment are based on systemic or intralesional 56 administration of pentavalent antimonials according to the species 57

and the clinical symptoms (intravenous or intramuscular 20–50 mg 59 Sb(v)/kg weight/day for 30 days, or 1–3 ml under the edge of lesion 60 and entire lesion every 5–7 days for a total of 2–5 times [12], systemic 61 amphotericin B and pentamidine isothionate [13,14]. The response to 62 the treatment is slow and even inefficacious according to the species, 63 with incomplete cure and relapse occurring within 6 months [13]. 64 Treatments are linked to side effects such as hepatic alterations, 65 biochemical pancreatitis, flattening of T waves in ECG, myalgia, 66 arthralgia, thrombocytopenia, transient suppression of bone marrow 67 and reversible renal insufficiency [15]. 68

Thus, a search for an effective, simple, and low-cost treatment for 69 CL that can be administered conveniently is still an active topic. In this 70 scenario, topical treatment is preferable to systemic interventions 71 [16]. The highly hydrophilic antibiotic paromomycin ointment (15%) 72 associated to the permeation enhancer methyl benzethonium 73 chloride (12%) (MBC), are relatively effective for CL treatment (*L* 74 *major*, *L. tropica*, *L. mexicana* and *L. panamensis*), but local side effects 75 are observed frequently due to MBC [17]. On the other hand, topical 76 amphotericin B (Amphocil in 5% ethanol) has been successful in 77 treatment of *L. major* infected patients in Israel [18,19], but the high 78 cost of Amphocil restricts the use to patients and more extensive 79 studies are needed. 80

\* Corresponding author. Tel.: +54 1143657100; fax: +54 1143657132.

E-mail address: [elromero@unq.edu.ar](mailto:elromero@unq.edu.ar) (E.L. Romero).

Photodynamic therapy (PDT) is a potentially applicable, safe and affordable technology that is currently in use for the treatment of cancer and aged-related macular degeneration. PDT is based on the concept that a photoactivatable compound, called a photosensitizer, can be excited by light of the appropriate wavelength to generate cytotoxic singlet oxygen and free radicals [20]. PDT is an attractive option to conventional antimicrobial chemotherapy, since it does not induce resistant strains neither upon multiple treatments [21,22]. Although PDT has rendered several cases of CL clinical cure with good cosmetic results [23,24], the lack of standardized data and the needs for special medical equipment (lamps), have hampered the use of PDT against CL [25]. The use of daylight to PDT can be an alternative to this last drawback. Recently a Phase II clinical trial in Israel has been started to determine the efficiency of methyl aminolevulinate (MAL)-PDT daylight triggered for the treatment of CL (*L. major* and *L. tropica*) [26].

In the present work, we have determined the *in vitro* leishmanicidal activity of the hydrophobic photosensitizer Zn phthalocyanine (ZnPc) loaded in ultradeformable liposomes (UDL-ZnPc) both in the darkness and upon sunlight irradiation and screened the ability of UDL-ZnPc to penetrate intact skin.

## 2. Materials and methods

### 2.1. Materials

Soybean phosphatidylcholine (SPC) (phospholipon 90 G, purity >90%) was a gift from Phospholipid/Natterman, Germany. Sodium cholate (NaChol), 1,2-Dimyristoyl-*sn*-glycero-3-phosphoethanolamine-N-(Lissamine™ rhodamine B sulfonyl) (Rh-PE), and Sephadex G-50 were purchased from Sigma-Aldrich, Argentina. The fluorophore 8-hydroxypyrene-1,3,6-trisulfonic acid (HPTS) was from Molecular Probes (Eugene, OR, USA). Q-tracker non-targeted Quantum Dots 655, with a *core/shell* of CdSe/ZnS covered by PEG (QD) was from Invitrogen (Hayward, CA). The hydrophobic ([tetrakis(2,4-dimethyl-3-pentyloxi)-phthalocyaninate]zinc(II)) Zn phthalocyanine (ZnPc) was synthesized as described in Montanari et al. [27]. Other reagents were analytic grade from Anedra, Argentina.

### 2.2. Preparation and characterization of ultradeformable liposomes

UDL and UDL-ZnPc were prepared as stated in Montanari et al. [27]. Briefly, UDL composed of SPC and NaChol at 6:1 (w/w) ratio, were prepared by mixing lipids from CHCl<sub>3</sub> and CHCl<sub>3</sub>:CH<sub>3</sub>OH (1:1, v/v) solutions, respectively, that were further rotary evaporated at 40 °C in round bottom flask until organic solvent elimination. The thin lipid film was flushed with N<sub>2</sub>, and hydrated in 10 mM Tris-HCl buffer plus 0.9% (w/v) NaCl, pH 7.4 (Tris buffer), up to a final concentration of 43 mg SPC/ml. The suspension was sonicated (45 min with a bath type sonicator 80 W, 40 kHz) and extruded 15 times through two stacked 0.2 and 0.1 μm pore size polycarbonate filters using a 100 ml Thermobarrel extruder (Northern Lipids, Canada). ZnPc was co-solubilized in the organic solution with lipids (2 mg ZnPc/g SPC) to prepare UDL-ZnPc.

Conventional – non ultradeformable, without NaChol – liposomes (L) were prepared by the same procedure.

Liposomal phospholipids were quantified by a colorimetric phosphate micro assay [28]. Mean particle size of each liposomal preparation was determined by dynamic light scattering with Nanozetasizer (Malvern).

### 2.3. Cytotoxicity on mammal cells

#### 2.3.1. Lactate dehydrogenase (LDH) assay

J-774 and Vero cells were maintained at 37 °C with 5% CO<sub>2</sub>, in RPMI 1640 medium supplemented with 10% heat-inactivated FCS, 2 mM

glutamine, 100 UI/ml penicillin and 100 μg/ml streptomycin (PE/ST) and amphotericin (all from Invitrogen Corporation). Culture medium of nearly confluent cell layers was replaced by 100 μl of medium containing UDL (1 and 10 mM phospholipids). Upon 1 h incubation at 37 °C, suspensions were removed; cells were washed with PBS (140 mM NaCl, 8.7 mM Na<sub>2</sub>HPO<sub>4</sub>, 1.8 mM NaH<sub>2</sub>PO<sub>4</sub>, pH 7.4) replaced by fresh RPMI medium and cells were incubated for 24 h at 37 °C. Upon incubation, supernatants were transferred to fresh tubes; centrifuged at 250 ×g for 4 min and LDH content was measured using lactate dehydrogenase CytoTox Kit (Promega) [29]. LDH concentration was expressed as percentage LDH release relative to treatment with the detergent Triton X-100 and then percentage of viability was calculated considering the LDH leakage of cells grown in medium.

#### 2.3.2. Glutathione assay (GSH)

Total cellular glutathione of was measured using the Tietze method [30]. Culture medium of nearly confluent J774 cells was replaced by 100 μl of medium containing free ZnPc (1.25 and 12.5 μM), UDL (1 and 10 mM) UDL-ZnPc (1.25 μM ZnPc–1 mM phospholipids and 12.5 μM ZnPc–10 mM phospholipids). Upon 24 h at 37 °C incubation, suspensions were removed, replaced by fresh RPMI medium and one plate was exposed to direct sunlight along 15 min (light dose of 15 J/cm<sup>2</sup> at λ = 600–650 nm measured by Radiometer Laser Mate Q, Coherent), meanwhile other plate was kept in the dark. After treatments, cell cultures were incubated for 24 h at 37 °C, media were removed and cells were washed in PBS and collected into eppendorf tubes by trypsin treatment. Then trypsin was inactivated, cells were twice washed in PBS by centrifugation and finally suspended in 100 μl of 1 mM EDTA. Cells were lysed by sonication (tip sonicator 10 s) and cellular debris was removed by centrifugation (10000 ×g for 15 min at 4 °C). 20 μl aliquots of each supernatant were transferred to 96 wells plate for glutathione determination. The reaction was started by adding 180 μl of reaction mixture [60 μM 5,5'-dithio-bis(2-nitrobenzoic acid) (DTNB), 1.5 mM NADPH, 0.1 mM EDTA, and 2.4 U/ml GSH reductase in NaHCO<sub>3</sub> 0.1% (all from Sigma-Aldrich, St. Louis, MO, USA)]. Absorbance at 412 nm was monitored after 15 min with microplate reader and the glutathione concentration was determined by comparing the rate of colour change with that of a GSH standard curve.

### 2.4. UDL-ZnPc internalization by promastigotes

*Leishmania braziliensis* promastigotes (STRAIN 2903) were cultured at 25 °C in Novy–McNeal–Nicolle biphasic medium [31] and RPMI 1640 supplemented with 10% FCS and PE/ST. Before treatments, promastigotes were taken from liquid phase and transfer to RPMI medium.

*L. braziliensis* promastigotes were incubated with UDL-ZnPc (1.25 μM ZnPc–1 mM phospholipids) for 15 min at 4 °C and 25 °C. Upon incubation, parasites were washed by centrifugation (3830 ×g for 3 min) and fixed in 2% v/v formaldehyde in PBS. The emission of ZnPc was monitored with a confocal laser scanning microscope (CLSM) Olympus FV300 equipped with a He–Ne 633 nm laser.

### 2.5. Anti-promastigote activity

Promastigotes were incubated for 5 min at 25 °C with empty L and UDL (1 and 0.1 mM phospholipids) (100 μl RPMI with 10% FCS and PE/ST). Upon incubation, samples were centrifuged (3800 ×g for 10 min at 20 °C), supernatants were removed and replaced by fresh RPMI medium. Parasites were further incubated for 3 h at 25 °C and mobility was evaluated microscopically.

Promastigotes (5 × 10<sup>5</sup>) were incubated for 30 min at 25 °C with empty UDL (1 mM phospholipids), free ZnPc (1.25 μM), UDL-ZnPc and L-ZnPc (both 1.25 μM ZnPc–1 mM phospholipids). Upon

incubation, samples were centrifuged (3800×g for 10 min at 20 °C), supernatants were removed and replaced by fresh RPMI medium, and exposed 15 min to direct sunlight as stated before. Control cells were maintained on the dark. After treatments, parasites were incubated at for 24 h or 48 h at 25 °C and inhibition of promastigotes growth was microscopically determined by counting parasite numbers in a Neubauer haemocytometer. Anti-promastigote activity was expressed as: % APA = [1 – (no. of promastigotes treated)/(no. of promastigotes control)] × 100.

## 2.6. Intracellular anti-amastigote activity

RAW macrophages maintained in RPMI 1640 medium supplemented with 10% FCS and PE/ST were infected with *Leishmania* promastigotes at 1:10 macrophage: promastigotes ratio, and the following treatments were done: a. 24 h incubation with UDL-ZnPC (1.25 μM ZnPC–1 mM phospholipids) or ZnPC (1.25 μM); b. 2 h incubation with UDL-ZnPC, ZnPC or empty UDL followed by 22 h incubation in RPMI medium; c. 22 h incubation only with promastigotes followed by 2 h incubation with UDL-ZnPC or ZnPC. After incubation in the dark, suspensions were removed, replaced by fresh RPMI medium and exposed to direct sunlight along 15 min as described above. Control cells were maintained on the dark. After 24 h, the coverslips were removed, washed with PBS, fixed with methanol and stained with Giemsa. The number of amastigotes/300 cells was counted by using light microscopy. Untreated infected macrophages were used as control. Anti-amastigote activity was expressed as: % AA = [1 – (no. of amastigotes/100 cells) treated/(no. of amastigotes/100 cells) control] × 100.

## 2.7. In vitro skin penetration studies

Excised human skin from Caucasian female patients, who had undergone abdominal plastic surgery, was used. Patients were healthy and with no medical history of dermatological disease. After excision, the skin was cut into 10 × 10 cm<sup>2</sup> pieces and the subcutaneous fatty tissue was removed from the skin specimen using a scalpel. Afterwards the surface of each specimen was cleaned with water, wrapped in aluminum foil and stored in polyethylene bags at –26 °C until use. Previous investigations have shown that no change in the penetration characteristics occurs during the storage time of 6 months [32,33].

Disks of 24 mm in diameter were punched out from frozen skin, thawed, cleaned with PBS solution, and transferred directly into the Saarbrücken Penetration model (SPM). Briefly, the skin was put onto a filter paper soaked with Ringer solution and placed into the cavity of a Teflon block.

UDL and L containing HPTS (UDL-HPTS and L-HPTS) were prepared as stated in Section 2.2, excepting that the lipid film was hydrated with a solution containing 35 mM HPTS Tris–HCl buffer. After extrusion the free HPTS was eliminated by gel permeation chromatography in a Shepadex G-50 column using minicolumn centrifugation method [34].

UDL-HPTS or L-HPTS (11 μl/cm<sup>2</sup> corresponding to 0.12 mg phospholipids/cm<sup>2</sup> and same amount of HPTS) were applied to the skin surface, the system was placed into an oven at 35 °C, and were incubated for 1 and 5 h after drying of the vesicle solutions. Besides, UDL-ZnPC, L-ZnPC and free ZnPC solubilized in DMSO were applied to the skin disks at 2.58 nmol of ZnPC/cm<sup>2</sup>, placed at 35 °C and incubated for 1 h after drying of the suspensions.

### 2.7.1. Skin segmentation

After incubation time the skin specimens mounted on SPM were segmented using tape stripping method or optically scanned by CLSM.

**2.7.1.1. Tape stripping.** After the incubation time skin specimens were segmented using tape stripping method as described by Wagner [35]. Briefly, the formulation was wiped off from the skin surface using cotton. Then the skin piece was mounted on an extruded polystyrene foam disc using small pins to stretch the tissue and covered with a teflon mask with a central hole of 15 mm in diameter for the HPTS formulations and successively stripped with 20 pieces of adhesive tape (Scotch 3 M) placed on the central hole, while for the ZnPC formulations the tapes were placed covering the whole surface of the skin segments. Each tape was charged with a weight of 2 kg per 10 s and rapidly removed.

HPTS was extracted from each tape with 3 ml of ethanol–water (1:1 v:v), shaken at 190 rpm for 1 h at 37 °C. Emission of HPTS (510 nm) was measured upon excitation at 453 nm, using a Perkin-Elmer LS 55 spectrofluorometer.

ZnPC from the twenty tapes was extracted overnight with 4 ml of DMSO at room temperature. Emission of ZnPC at 710 nm was measured upon excitation at 699 nm [36]. Calibration curves were prepared among each experiment to quantify the ZnPC, showing linear behavior between 0.01 and 0.2 μmol/l with a correlation coefficient (r<sup>2</sup>) of 0.999.

After the tape stripping, the remaining skin below the stratum corneum (SC) – i.e. the viable epidermis and the dermis – was cut into small pieces, placed into 4 ml of DMSO, homogenized, sonicated for 20 min, filtered and the fluorescence was measured the same as for the tapes [36].

**2.7.1.2. Optical scanning.** After incubation, the full skin thickness was optically scanned at 2 μm increments through the z-axis by CLSM equipped with an Ar laser (488 nm). Fluorescence intensity of each image was obtained by Image-J software.

### 2.7.2. Skin cryosectioning

UDL and L containing HPTS and Rh-PE or ZnPC (UDL-HPTS-Rh-PE/ZnPC and L-HPTS-Rh-PE/ZnPC) were prepared as stated in Section 2.2, excepting that Rh-PE (1: 1000, Rh-PE: SPC, mol:mol) or ZnPC were co-solubilized in organic solution with lipids. UDL containing Quantum Dots (UDL-QD) were prepared by hydration the thin lipid film with a suspension of 0.01 nmol QD/ml in Tris buffer. Negative staining electron microscopy images of liposomes upon uranyl acetate staining were obtained with a JEOL JEM 1200 EX II microscope.

Formulations were applied to the skin surface and incubated for 1 h in a SPM as stated before (Section 2.7). After incubation the skin was rapidly frozen in dry ice, embedded in OCT and sliced in sections of 8 μm thickness, perpendicular to the skin, with a cryomicrotome Reichert-Jung CryoCut 1800 (Germany). Skin slices were fixed with 10% formaldehyde and observed by CLSM equipped with an Ar laser (488 nm for HPTS and QD excitation) and a He–Ne laser (543 nm for Rh-PE and ZnPC excitation).

The same specimens were also subjected to hematoxylin and eosin staining in order to detect using light microscopy the possible presence of histological alterations in the analyzed tissues.

## 2.8. Statistical analysis

The significance of the differences between the mean values of studied parameters was determined using the Student's *t*-test.

## 3. Results

### 3.1. Size and z potential

The preparations rendered UDL-ZnPC (58 nmol ZnPC/52 μmol phospholipid/ml) of 99.9 ± 1.2 nm in size with unimodal distribution and a Zeta potential of –36.7 ± 3.8. Similar results were obtained for L-ZnPC (44 nmol ZnPC/44 μmol phospholipid/ml).



## 319 3.2. Cytotoxicity on mammal cells

320 The effect of empty UDL on cell membrane integrity of fibroblasts  
 321 (Vero cells) and of macrophages (J-774 cells) was determined by LDH  
 322 leakage. UDL at 1 mM phospholipids did not induce LDH leakage on  
 323 both cell types, although at 10 mM caused 80% leakage of LDH on J774  
 324 cells upon 1 h incubation (Fig. 1a). L did not produce LDH leakage  
 325 either at 1 or 10 mM (data not shown). Additionally, total GSH level in  
 326 J774 cells was measured upon incubation with UDL-ZnPc followed by  
 327 sun irradiation. GSH level was not altered after incubation with free  
 328 ZnPc, empty UDL and UDL-ZnPc (1 mM phospholipids–1.25  $\mu$ M ZnPc)  
 329 in the dark or after irradiation. Although, GSH was significantly  
 330 diminished upon incubation at 10 mM phospholipids–12.5  $\mu$ M ZnPc  
 331 followed by 15 min of sun irradiation (Fig. 1b). 12.5  $\mu$ M free ZnPc and  
 332 10 mM empty UDL did not affected GSH level.

## 333 3.3. UDL-ZnPc internalization by promastigotes

334 *L. braziliensis* promastigotes were incubated with UDL-ZnPc at  
 335 25 °C (optimum temperature of growth) and at 4 °C (temperature at  
 336 which internalization by endocytic uptake is absent due to reduced  
 337 metabolism of cells [37]) to distinguish between active uptake and  
 338 superficial adsorption. Fluorescence microscopy showed higher  
 339 intensity of fluorescence upon incubation at 25 °C than at 4 °C  
 340 (Fig. 2). These results could suggest that UDL-ZnPc were internalized  
 341 by promastigotes by endocytic uptake.

## 342 3.4. Anti-promastigote activity

343 First, it was observed that around 17 and 29% of promastigotes lost  
 344 motility upon incubation with L at 0.1 and 1 mM, respectively, while  
 345 the rest of the parasites kept highly mobile. Although, 5 min  
 346 incubation with UDL induced an important diminish of motility. 90%  
 347 of parasites lost motility after incubation with UDL at 0.1 and 1 mM,

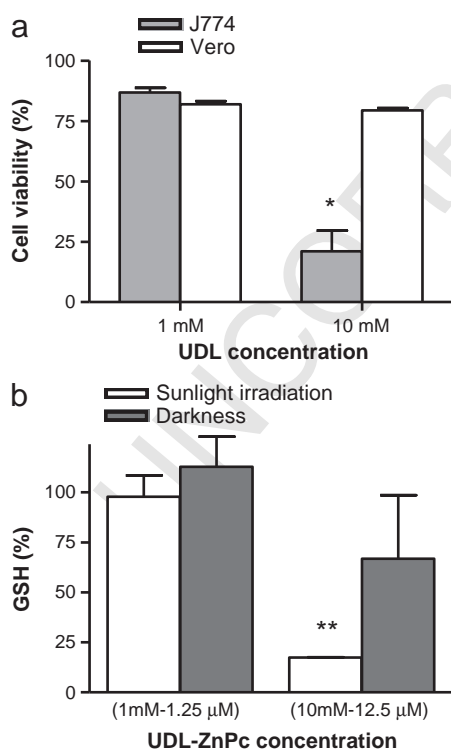


Fig. 1. Mammal cells cytotoxicity measured as LDH leakage induced by UDL on J774 and Vero cells upon 1 h incubation (a) and GSH content in J774 cells after incubation with UDL-ZnPc in the dark or upon irradiation (b). Each data point represents the mean  $\pm$  standard deviation ( $n=3$ ). \* $p<0.05$ , \*\* $p<0.01$ .

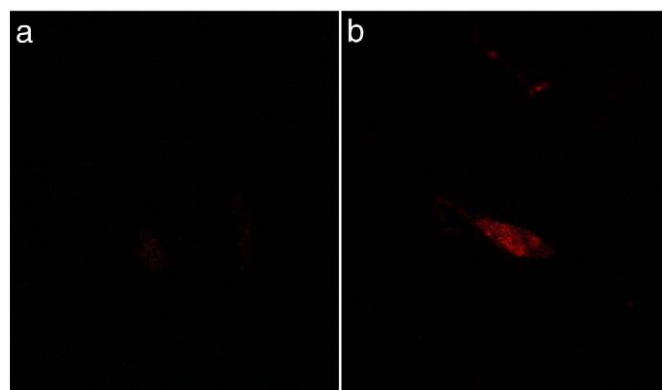


Fig. 2. CLSM images of *L. braziliensis* promastigotes incubated with UDL-ZnPc at 4 °C (a) and 25 °C (b).

meanwhile the rest of the parasites kept highly mobile (0.1 mM) or 348  
 with low motility (1 mM). 349

Then, to determine if lost of motility were related with loss of 350  
 viability, anti-promastigote activity (APA) was determined after 351  
 30 min incubation followed by 24 or 48 h of parasite growth. First, 352  
 empty UDL and UDL-ZnPc in the dark showed high and similar APA of 353  
 around 80% after 24 h of growth. Nevertheless, the highest anti- 354  
 promastigote effect (100% APA) was shown upon 15 min of sun 355  
 irradiation of promastigotes treated with UDL-ZnPc (Fig. 3). Upon 356  
 48 h of parasite growth, the all the treatments showed APA of around 357  
 100%. 358

On the other hand, free ZnPc at 1.25  $\mu$ M did not affect the motility 359  
 of promastigotes upon 5 min incubation and it showed a 20% APA 360  
 after sun irradiation and 48 h of parasite growth, while L-ZnPc 361  
 showed 0% APA in the darkness or upon irradiation (data not shown). 362

## 363 3.5. Intracellular anti-amastigote activity

Anti-amastigote activity (AA) was determined in two ways: first, 364  
 samples were co-incubated for 2 or 24 h with RAW macrophages and 365  
 promastigotes and second, samples were incubated for 2 h with 366  
 macrophages previously infected. 367

Empty UDL had insignificant AA (5%), meanwhile activity of free 368  
 ZnPc and UDL-ZnPc increased as time of incubation increased from 2 369  
 to 24 h (Fig. 4a). While free ZnPc showed activity only upon 370  
 irradiation (20 and 35% AA after 2 and 24 h, respectively), when 371  
 incorporated in UDL (UDL-ZnPc) activities in the dark or upon 372  
 irradiation were not different (AA 40 and 80% after 2 and 24 h, 373  
 respectively), but were almost the double of AA for free ZnPc. 374

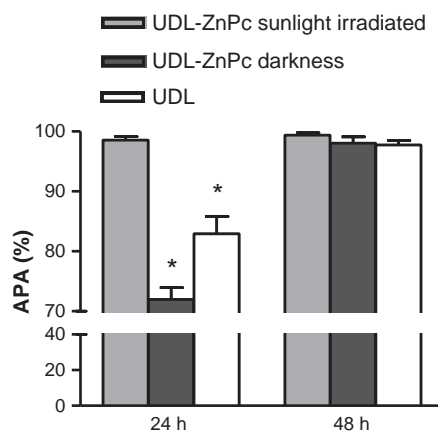
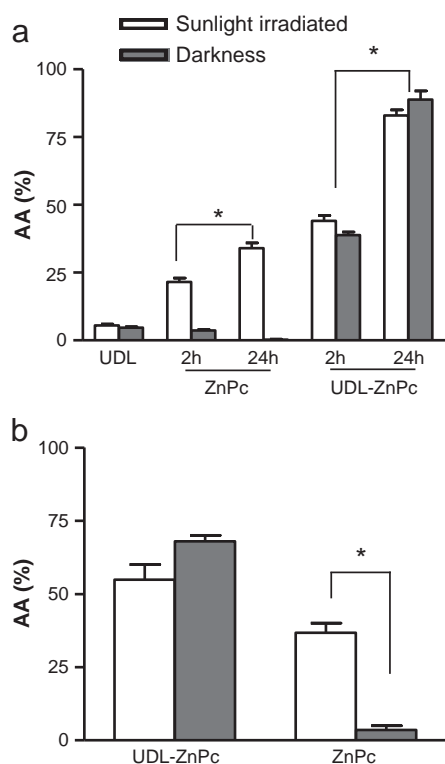


Fig. 3. Anti-promastigote activity (APA%) of UDL and UDL-ZnPc in the dark or upon 15 min sunlight irradiation. \* $p<0.05$ .



**Fig. 4.** Anti-amastigote activity (AA%) of UDL, ZnPc and UDL-ZnPc co-incubated with RAW macrophages and *L. braziliensis* promastigotes for 2 or 24 h (a), and of UDL-ZnPc and ZnPc incubated with RAW macrophages previously infected with *L. braziliensis* promastigotes for 2 h (b). Cells were then exposed to 15 min sunlight irradiation or maintained in the dark and grown for 24 h. \* $p < 0.05$ .

Finally, free ZnPc as well as UDL-ZnPc showed AA upon 2 h incubation with infected macrophages (Fig. 4b). Again, free ZnPc activity was irradiation dependent (3 vs 36% AA, in the dark and after irradiation, respectively), while UDL-ZnPc activity was independent (55% AA) and higher than AA for free ZnPc.

### 3.6. In vitro skin penetration studies

Skin penetration of the hydrosoluble fluorescent dye HPTS encapsulated in UDL and L was determined using the SPM followed by segmentation by tape stripping or optical scanning by CLSM up to 60  $\mu\text{m}$  depth. The presence of ZnPc in SC and in deeper viable epidermis and dermis upon incubation as free ZnPc, UDL-ZnPc and L-ZnPc was also quantified. Finally, skin penetration of HPTS and the hydrophobic Rh-PE or ZnPc co-encapsulated in UDL and L were recorded by cryosectioning to assess the integrity of vesicles along penetration.

SPM was employed under non-occlusive conditions, in order to maintain the humidity gradient across the skin, that it is proposed to be the locomotive force for UDL penetration [38]. If compared with Franz diffusion cell, SPM avoids the non-physiological hydration and changes of the skin due to the absence of liquid as receptor medium. This system, coupled to segmentation techniques, such as tape stripping or cryosectioning, allows the measurement of penetration profiles of drugs with respect to the depth of the tissue. To avoid the reported variability of the tape stripping [39–41], the experiments were carried out with the same skin donor, repeated 5 times and the distance and geometry of skin fixation – responsible for maintaining the stretching of the skin during tape stripping – were kept constant.

Fluorescence profiles of UDL-HPTS and L-HPTS extracted from each strip upon 1 h incubation were significantly different (Fig. 5). The cumulative of fluorescence in the 20 strips (corresponding to the total SC), was around 6.8 folds higher for UDL-HPTS than for L-HPTS

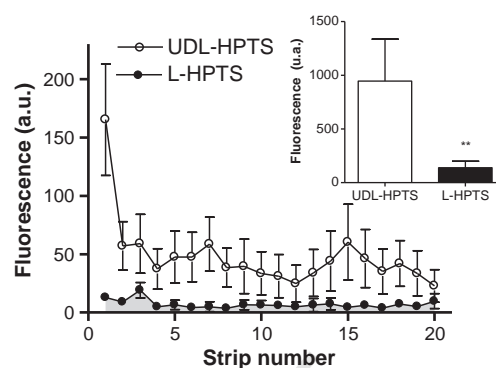


**Fig. 5.** SC strip profile of HPTS after 1 h of non-occlusive application of UDL-HPTS or L-HPTS ( $n = 5$ ). Inset: Cumulative fluorescence in the 20 strips. \*\* $p < 0.01$ .

(Inset Fig. 5). Fluorescence profiles and accumulated fluorescence upon 5 h incubation were similar to those obtained after 1 h of incubation, for both formulations.

In this procedure, each removed cell layer had nearly the same thickness [35,42] being the number of tape strips linearly correlated with the remaining thickness of the SC. According to this, UDL-HPTS penetrated deeper into the SC than L-HPTS.

The optical scanning (Fig. 6) showed that HPTS distributed in SC layers in patterns similar, but slightly thicker than the net of nanochannels previously described [43,44].

The use of SPM ensured that the detected fluorescence was exclusively owed to the penetration of HPTS, Rh-PE or ZnPc from top to bottom at the lower layers of the epidermis, and not to the basolateral penetration which is inherent to the Franz cell [35].

Transversal skin cryosections after 1 h incubation with double fluorescently labeled liposomes (UDL-HPTS-Rh-PE/ZnPc or L-HPTS-Rh-PE/ZnPc), showed maximal fluorescence intensity of Rh-PE/ZnPc from UDL at the first 8  $\mu\text{m}$  up to a depth of 14  $\mu\text{m}$ , in the boundaries of the viable epidermis (8–13  $\mu\text{m}$  [45]). Based on the osmotic force theory of Cevc and Blume [46], the UDL would not penetrate beyond the non-hydrated deepest layers of the SC. The hydrophilic HPTS

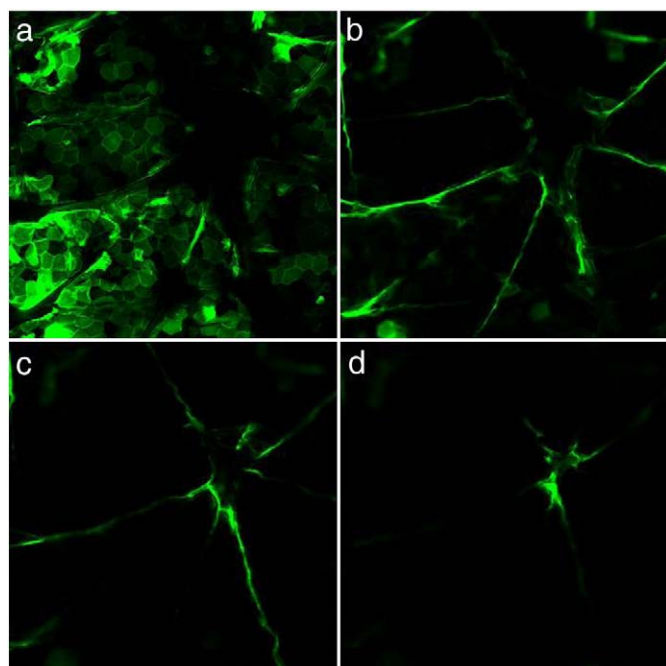
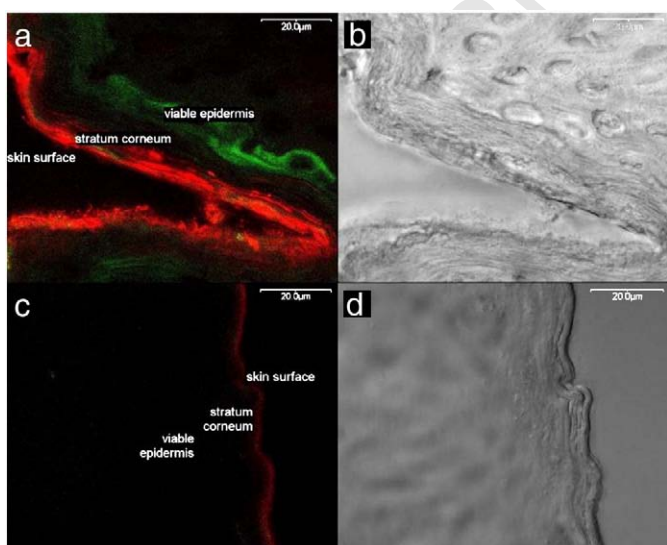


**Fig. 6.** Typical series of CLSM images obtained horizontally at 0  $\mu\text{m}$  (a), 20  $\mu\text{m}$  (b), 40  $\mu\text{m}$  (c) and 60  $\mu\text{m}$  (d) from skin surface upon 1 h incubation with UDL-HPTS.

427 however, was found in a separate fraction, entering the viable  
 428 epidermis, up to a mean depth of 24  $\mu\text{m}$  (Fig. 7a and b). On the  
 429 contrary, fluorescence of Rh-PE/ZnPc from L was only detected at the  
 430 first 1  $\mu\text{m}$  (first SC cells layer), while a slight diffuse poorly intense  
 431 fluorescence from HPTS was found up to 2  $\mu\text{m}$  (Fig. 7c and d).

432 After 1 h incubation in SPM of 11.7 nmol ZnPc (dissolved in  
 433 DMSO at 0.98  $\mu\text{mol}/\text{ml}$ )/4.5  $\text{cm}^2$  total area, followed by removal of  
 434 material remaining on the skin surface, it was found that only 1 out  
 435 of 5 skin samples contained ZnPc in quantitative amounts within SC,  
 436 viable epidermis and dermis (data not shown). On the contrary,  
 437 upon applying the same amount of ZnPc/4.5  $\text{cm}^2$  either as UDL-ZnPc  
 438 or L-ZnPc, it was found that UDL-ZnPc delivered 7.35 folds higher  
 439 amount of ZnPc than L-ZnPc. As judged by the penetration profile of  
 440 Rh-PE/ZnPc in Fig. 7 it was reasonably to assume that the UDL-ZnPc  
 441 (lipid matrix and ZnPc) homogeneously distributed across the  
 442  $\sim 8 \mu\text{m}$  thickness of the SC, whereas L-ZnPc remained stacked on  
 443 the first layer of the SC. In other words, upon applying the same  
 444 amount ZnPc/surface,  $\sim 3.8 \times 10^{-2}$  nmol UDL-ZnPc were evenly  
 445 distributed in a volume of [1  $\text{cm}^2$  surface  $\times 8 \times 10^{-4}$  cm depth] of  
 446 SC, while  $\sim 5.4 \times 10^{-3}$  nmol L-ZnPc distributed in a volume of [1  $\text{cm}^2$   
 447 surface  $\times 1 \times 10^{-4}$  cm depth]. Hence, UDL-ZnPc rendered nearly 7  
 448 more ZnPc within the SC, distributed in a cylinder 8 fold more  
 449 profound than L-ZnPc. Assuming a homogeneous distribution, the  
 450 concentration of UDL-ZnPc within the whole depth of SC was 47  $\mu\text{M}$ ,  
 451 far beyond the concentration that *in vitro* was necessary to kill  
 452 promastigotes upon 15 min sunlight irradiation. UDL-ZnPc also  
 453 rendered nearly 40 folds higher amount ZnPc ( $8.63 \times 10^{-3}$  nmol)  
 454 distributed across the reminder viable epidermis and dermis, than L-  
 455 ZnPc (Fig. 8). Again, only 1 out of 5 skins showed a significant  
 456 presence of ZnPc within the rest of skin when it was applied in DMSO  
 457 solution (data not shown).

458 Finally, the penetration profile of QD and UDL-QD was determined.  
 459 The UDL-QD suspension was translucent with a mean vesicular size of  
 460 102 nm and polydispersity index of 0.128 (Fig. 9a and b). After 1 h  
 461 incubation, the fluorescence of QD was distributed both across the SC  
 462 as well across the viable epidermis (Fig. 10a) in coincidence with  
 463 other authors [47], whereas that of UDL-QD remained confined in the  
 464 thickness of the SC (Fig. 10b).



465  
 466  
 467  
 468  
 469  
 470  
 471  
 472  
 473  
 474  
 475  
 476  
 477  
 478  
 479  
 480  
 481  
 482  
 483  
 484  
 485  
 486  
 487  
 488  
 489  
 490  
 491  
 492  
 493  
 494  
 495  
 496  
 497  
 498  
 499  
 500  
 501  
 502  
 503  
 504  
 505  
 506  
 507  
 508  
 509  
 510  
 511  
 512  
 513  
 514  
 515  
 516  
 517  
 518  
 519  
 520  
 521  
 522  
 523  
 524  
 525  
 526  
 527  
 528  
 529  
 530  
 531  
 532  
 533  
 534  
 535  
 536  
 537  
 538  
 539  
 540  
 541  
 542  
 543  
 544  
 545  
 546  
 547  
 548  
 549  
 550  
 551  
 552  
 553  
 554  
 555  
 556  
 557  
 558  
 559  
 560  
 561  
 562  
 563  
 564  
 565  
 566  
 567  
 568  
 569  
 570  
 571  
 572  
 573  
 574  
 575  
 576  
 577  
 578  
 579  
 580  
 581  
 582  
 583  
 584  
 585  
 586  
 587  
 588  
 589  
 590  
 591  
 592  
 593  
 594  
 595  
 596  
 597  
 598  
 599  
 600  
 601  
 602  
 603  
 604  
 605  
 606  
 607  
 608  
 609  
 610  
 611  
 612  
 613  
 614  
 615  
 616  
 617  
 618  
 619  
 620  
 621  
 622  
 623  
 624  
 625  
 626  
 627  
 628  
 629  
 630  
 631  
 632  
 633  
 634  
 635  
 636  
 637  
 638  
 639  
 640  
 641  
 642  
 643  
 644  
 645  
 646  
 647  
 648  
 649  
 650  
 651  
 652  
 653  
 654  
 655  
 656  
 657  
 658  
 659  
 660  
 661  
 662  
 663  
 664  
 665  
 666  
 667  
 668  
 669  
 670  
 671  
 672  
 673  
 674  
 675  
 676  
 677  
 678  
 679  
 680  
 681  
 682  
 683  
 684  
 685  
 686  
 687  
 688  
 689  
 690  
 691  
 692  
 693  
 694  
 695  
 696  
 697  
 698  
 699  
 700  
 701  
 702  
 703  
 704  
 705  
 706  
 707  
 708  
 709  
 710  
 711  
 712  
 713  
 714  
 715  
 716  
 717  
 718  
 719  
 720  
 721  
 722  
 723  
 724  
 725  
 726  
 727  
 728  
 729  
 730  
 731  
 732  
 733  
 734  
 735  
 736  
 737  
 738  
 739  
 740  
 741  
 742  
 743  
 744  
 745  
 746  
 747  
 748  
 749  
 750  
 751  
 752  
 753  
 754  
 755  
 756  
 757  
 758  
 759  
 760  
 761  
 762  
 763  
 764  
 765  
 766  
 767  
 768  
 769  
 770  
 771  
 772  
 773  
 774  
 775  
 776  
 777  
 778  
 779  
 780  
 781  
 782  
 783  
 784  
 785  
 786  
 787  
 788  
 789  
 790  
 791  
 792  
 793  
 794  
 795  
 796  
 797  
 798  
 799  
 800  
 801  
 802  
 803  
 804  
 805  
 806  
 807  
 808  
 809  
 810  
 811  
 812  
 813  
 814  
 815  
 816  
 817  
 818  
 819  
 820  
 821  
 822  
 823  
 824  
 825  
 826  
 827  
 828  
 829  
 830  
 831  
 832  
 833  
 834  
 835  
 836  
 837  
 838  
 839  
 840  
 841  
 842  
 843  
 844  
 845  
 846  
 847  
 848  
 849  
 850  
 851  
 852  
 853  
 854  
 855  
 856  
 857  
 858  
 859  
 860  
 861  
 862  
 863  
 864  
 865  
 866  
 867  
 868  
 869  
 870  
 871  
 872  
 873  
 874  
 875  
 876  
 877  
 878  
 879  
 880  
 881  
 882  
 883  
 884  
 885  
 886  
 887  
 888  
 889  
 890  
 891  
 892  
 893  
 894  
 895  
 896  
 897  
 898  
 899  
 900  
 901  
 902  
 903  
 904  
 905  
 906  
 907  
 908  
 909  
 910  
 911  
 912  
 913  
 914  
 915  
 916  
 917  
 918  
 919  
 920  
 921  
 922  
 923  
 924  
 925  
 926  
 927  
 928  
 929  
 930  
 931  
 932  
 933  
 934  
 935  
 936  
 937  
 938  
 939  
 940  
 941  
 942  
 943  
 944  
 945  
 946  
 947  
 948  
 949  
 950  
 951  
 952  
 953  
 954  
 955  
 956  
 957  
 958  
 959  
 960  
 961  
 962  
 963  
 964  
 965  
 966  
 967  
 968  
 969  
 970  
 971  
 972  
 973  
 974  
 975  
 976  
 977  
 978  
 979  
 980  
 981  
 982  
 983  
 984  
 985  
 986  
 987  
 988  
 989  
 990  
 991  
 992  
 993  
 994  
 995  
 996  
 997  
 998  
 999  
 1000

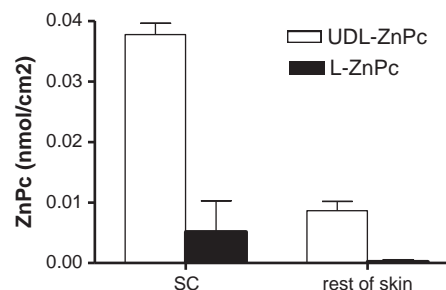


Fig. 8. Penetration of ZnPc in skin layers after 1 h non-occlusive incubation with UDL-ZnPc and L-ZnPc.

#### 4. Discussion

465

466 *In vitro*, aminolevulinic acid (ALA)-PDT fails in eliminate the  
 467 intracellular leishmania amastigotes. For instance, 4 h incubation with  
 468 ALA follow by irradiation with a 635 nm laser up to 50  $\text{J}/\text{cm}^2$  of *L major*  
 469 infected J774 cells, reduce the number of J774 cells but does not  
 470 diminish the number of intracellular parasites [48]. The reason for this  
 471 is that only mammal host cells can metabolize the ALA precursor to  
 472 the photosensitizer protoporphyrin IX (PpIX). PpIX is further  
 473 accumulated inside the intracellular amastigotes in an amount  
 474 insufficient to kill the parasites at fluence of 10  $\text{J}/\text{cm}^2$ . The phototoxic  
 475 effect against parasites occurs at a high concentration of PpIX  
 476 ( $\text{LD}_{50} \approx 3.8 \times 10^{-4}$  M), that cannot be applied *in vivo* without  
 477 generating serious toxic side effects. Clinically however, succeed  
 478 application of ALA- and MAL-PDT to CL patients caused by *L. donovani*  
 479 and *L. major*, have been published in 2003 and 2004 [49–51]. Recently,  
 480 it was shown that lesions healed rapidly with good cosmetics in a  
 481 patient with facial cutaneous *L. tropica* infection resistant to various  
 482 therapeutic regimens after MAL-PDT treatment [23] and improved  
 483 results were found in a comparative study between ALA-PDT and  
 484 topical paromomycin [52]. It is feasible that *in vivo* the induction of a  
 485 local immune response (for instance increased levels of IL-6) leading  
 486 to a non-specific tissue damage accompanied by macrophages  
 487 elimination, should account for the success of the ALA-PDT [48]. In  
 488 other words, the leishmanicidal effect is mediated by an immune host  
 489 reaction against a non-specific photochemical damage, and not by a  
 490 selective effect exclusively elicited by the PDT.

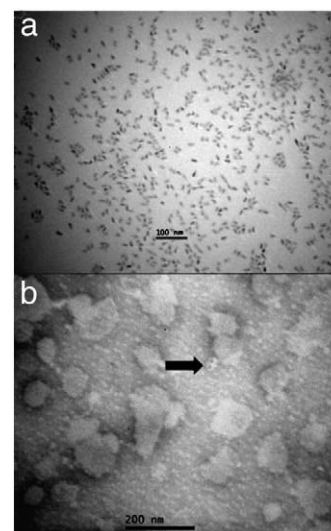
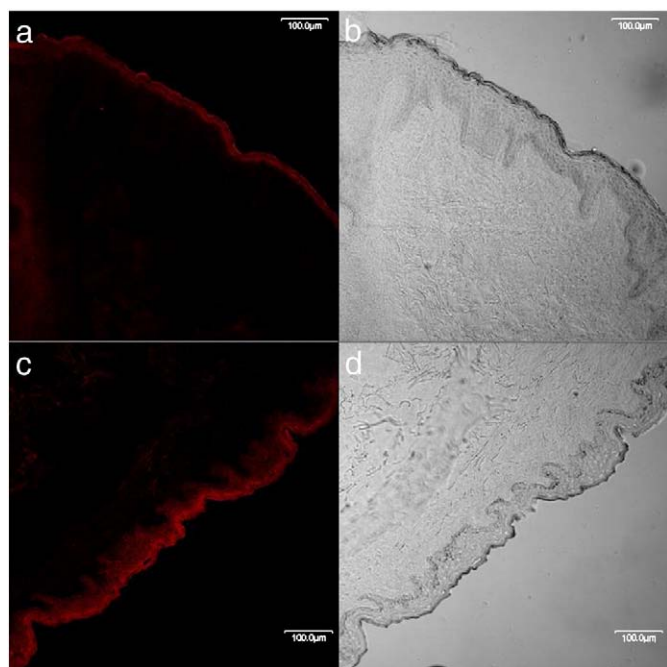


Fig. 9. Transmission electron microscopy images of free QD (a) (ellipsoidal shape, 6 nm short axis, 12 nm long axis and hydrodynamic diameter due to polyethylene glycol coverage up to 45 nm [68]) and UDL-QD (b). Arrow points to QD contained inside UDL.





**Fig. 10.** CLSM images of cryosectioned skin after 1 h of incubation with UDL-QD (a and b, fluorescence and the corresponding differential interference contrast image, respectively) and with QD (c and d, fluorescence and the corresponding differential interference contrast image, respectively).

491 Different photosensitizers such as phenothiazinium, aluminum  
492 chloride phthalocyanine and zinc phthalocyanine (with direct action  
493 in their intact form), also have shown succeeding preclinical results in  
494 the last four years [53,54]. In particular, results from Dutta indicates  
495 that promastigotes and axenic amastigotes of *L. amazonensis* are more  
496 sensitive than J774 macrophages to light mediated cytolysis at low  
497 concentration (1  $\mu\text{M}$ ) of the hydrophobic aluminum phthalocyanine  
498 chloride (AlPhCl) under a low energy dose (1.5  $\text{J}/\text{cm}^2$ ). Nevertheless,  
499 AlPhCl had no AA on infected J774 cells, and intracellular amastigotes  
500 could be eliminated only when AlPhCl was previously incubated with  
501 axenic amastigotes before the macrophages were infected [55]. This  
502 fact suggested that the cell membrane could hinder the free access of  
503 AlPhCl to intracellular targets.

504 A suitable delivery system could help to overcome the tissue and  
505 cellular barriers interposed between hydrophobic phthalocyanines  
506 and target amastigotes. Actually, the co-localization of phthalocyanine  
507 and target in a small volume of space should be the key to optimize  
508 the photodynamic activity, because of the short half life (<0.1 ms) and  
509 small action radii (10–20 nm) of singlet oxygen [56]. However,  
510 changing both the internalization mechanism and the intracellular  
511 traffic of the phthalocyanine (free phthalocyanine diffuse across the  
512 plasma membrane, and then relocate to other intracellular mem-  
513 branes [57]) by means of a delivery system could also arise  
514 unexpected toxic effects.

515 With the aim of improving the penetration of the hydrophobic  
516 ZnPc across the intact SC without using organic solvents and to count  
517 on a particulate vehicle with increased chances of being selectively  
518 captured by infected macrophages in the skin, we had previously  
519 characterized and determined the photochemical parameters of ZnPc  
520 loaded in a highly hydrophilic ultradeformable lipid matrix. When  
521 partitioned in UDL bilayers, ZnPc remains in monomeric form and  
522 exhibit similar photodynamic properties than in organic solvents, as  
523 judged by the similar value of the singlet oxygen quantum yield from  
524 UDL-ZnPc and ZnPc in ethanol. Upon UDL-ZnPc internalization, the  
525 phago/lysosomal compartment of macrophages remains intact after  
526 15 min of sunlight irradiation. Cytotoxicity, as measured by the MTT  
527 assay on Vero and J774 cells, is absent up to 10  $\mu\text{M}$  free ZnPc, as well as

for up to 18 mM empty UDL, both in the dark or after 15 min sunlight  
irradiation. UDL-ZnPc at 10  $\mu\text{M}$  ZnPc–8 mM phospholipids however,  
reduces 75% J774 cell viability, not only after irradiation but also in the  
dark [27].

528  
529  
530  
531  
532 In this work the GSH levels and release of cytosolic LDH were  
533 tested to delimit a safe threshold concentration of UDL and UDL-ZnPc  
534 when incubated with host phagocytes. The crucial factors determin-  
535 ing the type of cell death following PDT are cell type, the subcellular  
536 localization of the photosensitizer, and the light dose applied [58]  
537 (lower doses – such as the one received upon 15 min sunlight  
538 irradiation – lead to more apoptotic cells, while higher doses result in  
539 more necrotic cells [59]). Diminished GSH (the principal intracellular  
540 low-molecular-weight thiol that plays a critical role in the cellular  
541 defence against oxidative and nitrosative stress in mammalian cells)  
542 levels are observed in the early stages of apoptosis [60]. We found that  
543 1.25  $\mu\text{M}$  free ZnPc or as UDL-ZnPc and 1 mM phospholipids empty  
544 UDL did not diminish the intracellular GSH level in J774 cells, neither  
545 in the darkness nor after 15 min sunlight irradiation. The presence of  
546 30 mol% of the detergent sodium cholate within the UDL matrix could  
547 induce membrane damages when in contact to host cell surface, but  
548 1 mM phospholipids empty UDL did not induce the release of LDH  
549 neither by Vero nor J774 cells. At 10 mM however, an important  
550 release of LDH was produced by J774 cells, which was absent at the  
551 same concentration of L phospholipids. The faster uptake rate of  
552 phagocytosis, leading to higher amounts of internalized detergent in  
553 comparison to endocytosis [61], could be the reason for this non-  
554 photodynamic damage caused by UDL on J774.

555 The leishmanicidal activity was tested at 1 mM phospholipids  
556 and 1.25  $\mu\text{M}$  ZnPc upon 15 min sunlight irradiation since neither  
557 photodynamic nor non-photodynamic damage as measured by MTT,  
558 LDH assays and GSH consumption by phagocytic cells was registered  
559 below these threshold concentrations. Only 5 min incubation at  
560 25  $^{\circ}\text{C}$  was sufficient for empty UDL to produce an important decrease  
561 in motility of promastigotes. Same sized L neither caused relevant  
562 effect on parasite motility nor was captured by promastigotes, in  
563 accordance with previous results indicating that submicron diam-  
564 eter L can only be absorbed on the surface of cell parasites [62]. The  
565 intense fluorescence signal from UDL-ZnPc associated to the parasite  
566 upon 15 min incubation at 25  $^{\circ}\text{C}$  suggested an active uptake of UDL.  
567 The cytoskeleton of *Leishmania* promastigote is organized as a  
568 microtubule network underlying the cell membrane. The only  
569 available area for exchange of macromolecules with the external  
570 environment is the nearly 1  $\mu\text{m}^2$  surface of the flagellar pocket  
571 [63,64]. The elastic modulus of UDL is twenty folds lower than that of  
572 L, allowing for micro/nanoscaled spontaneous fluctuations of the  
573 bilayer at room temperature [65]. This could facilitate its endocytic  
574 uptake by the flagellar pocket. Hence the lipid matrix ultradeform-  
575 ability leading to its internalization and parasite immobilization  
576 could be the source of the observed non-photodynamic leishmanicidal  
577 activity.

578 On the other hand, UDL-ZnPc showed 100% APA (five folds  
579 increased over that of free ZnPc) after 15 min sunlight irradiation.  
580 Both UDL-ZnPc in the darkness as well as empty UDL also exhibited  
581 around 80% APA, while ZnPc and L-ZnPc did not (this last even after  
582 sunlight irradiation). These facts indicated that a high APA could  
583 simply be induced by internalization of empty ultradeformable  
584 matrices. For UDL-ZnPc, the irradiation yet contributed to accelerate  
585 the leishmanicidal effect upon internalization.

586 As UDL-ZnPc, AA raised up to 80% (more than two folds increased  
587 over that of the strictly sunlight dependent AA of free ZnPc) when co-  
588 incubated with promastigotes and RAW macrophages along 24.  
589 Remarkably, AA of UDL-ZnPc was independent of irradiation. Part of  
590 the 80% AA could arise from APA caused by UDL/UDL-ZnPc before  
591 infecting the RAW cells. In other words, probably the observed AA  
592 aroused from an infection occurred with a lower amount of viable  
593 parasites that the stated in the experimental method.

Taken together, though formerly aimed for PDT, these results indicated that an important part of the UDL-ZnPc leishmanicidal activity was independent of the irradiation. As previously discussed, the empty ultradeformable lipid matrix was an effective non-photodynamic leishmanicidal agent that fully manifested as *in vitro* APA. The *in vitro* AA of UDL was absent, but the non-photodynamic AA from UDL-ZnPc was unexpectedly high. And explanation for this could be that phagocytosis of UDL-ZnPc by host cells resulted in products that were innocuous for the host but lethal for the parasites.

As previously observed by Cevc [38] and Honeywell–Nguyen [44], we determined that the hydrophobic Rh-PE or ZnPc and the hydrophilic HPTS when loaded in UDL rapidly entered the SC, but did not if loaded in L. Also in accordance to Honeywell–Nguyen [40,66] who determined that a hydrophilic drug is released from the lipid matrix diffusing to deeper layers in the epidermis, the hydrophobic molecules Rh-PE/ZnPc were found at the SC-viable epidermal junction, while HPTS was found deeper in the epidermis. At the end of the SC, the hydrophilic molecules were shuttled from the carrier.

Our results indicated that UDL-ZnPc penetrated homogeneously in the SC, carrying 7 folds higher amount of ZnPc 8 folds deeper than L-ZnPc while ZnPc in DMSO did it in a poorly reproducible fashion after 1 h incubation. Three weeks is the elapsed time for desquamation and renewal of SC [67] and probably within that period the UDL-ZnPc concentrated in SC would act as a reservoir for delivery of lipid matrix and ZnPc to the viable epidermis. Remarkably, the UDL-ZnPc was the only formulation ensuring a reproducible and quantitative delivery of ZnPc to the viable epidermis and dermis upon a single application and 1 h incubation. This amount could be increased after multiple applications. Infected macrophages can be found at different levels within the viable epidermis and clearly UDL-ZnPc showed to be a suitable tool to increase the amount of ZnPc delivered into and beyond the SC, as judged by this *in vitro* assay.

Infected macrophages are specialized in the uptake of particulate material. Hence the chances of being internalized should be increased as long as the vesicular integrity of UDL-ZnPc is conserved. Since the high sized ellipsoidal QD remained trapped into the relatively small (100 nm diameter) UDL matrix, probably the vesicular structure of the UDL were conserved along the SC penetration. Otherwise the QD should squeeze deeper into the epidermis, as the free QD did. Hence, excluding the use of organic solvents such as dimethylsulphoxide or dimethylformamide that are required to dissolve highly hydrophobic molecules like ZnPc, we could reasonably expect that in spite of the loss of hydrophilic content across the SC penetration, the ZnPc-UDL could get close to the viable epidermis in an – at least – partly particulate form.

Further studies will reveal if these UDL when applied in minimal doses on the surface of intact skin could have a preventive or therapeutic effect aroused both from their photodynamic activity as well as from their non-photodynamic activity during the first stages of the infection. It is likely that the leishmanicidal effect upon transcutaneous application of UDL could result from a synergistic effect fruit from its multiple leishmanicidal activity and its superior capacity of penetration.

## Acknowledgements

This work was supported by a grant from the Secretaria de Investigaciones, Universidad Nacional de Quilmes, and from the Comisión de Investigaciones Científicas de la Provincia de Buenos Aires. MJ Morilla and EL Romero are members of the Carrera del Investigador Científico del Consejo Nacional de Investigaciones Científicas y Técnicas, Argentina (CONICET). J. Montanari has got a fellowship from CONICET. Dr H Jimenez provided the skin explants from surgery. Students LA Lado and L Rivadeneyra collaborated in the development of the skin experiments.

## References

- R. Bonfante, S. Barruela, Leishmaniasis y Leishmaniasis en América con especial referencia a Venezuela, Tipografía y Litografía Horizonte C.A., Caracas, 2002.
- S. Jeronimo, A. de Queiroz Sousa, R. Pearson, in: R. Guerrant, D. Walker, P. Weller (Eds.), Tropical Infectious Diseases: Principles, Pathogens and Practice, Churchill Livingstone Elsevier, Edinburgh, Scotland, 2006, pp. 1095–1113.
- B.L. Herwaldt, Leishmaniasis, Lancet 354 (9185) (1999) 1191–1199.
- WHO, Leishmaniasis, 2004.
- C.R. Davies, E.A. Llanos-Cuentas, S.J. Sharp, J. Canales, E. Leon, E. Alvarez, N. Roncal, C. Dye, Cutaneous leishmaniasis in the Peruvian Andes: factors associated with variability in clinical symptoms, response to treatment, and parasite isolation rate, Clin. Infect. Dis. 25 (2) (1997) 302–310.
- C. Bern, J.H. Maguire, J. Alvar, Complexities of assessing the disease burden attributable to leishmaniasis, PLoS Negl. Trop. Dis. 2 (10) (2008) e313.
- E. Schwartz, C. Hatz, J. Blum, New world cutaneous leishmaniasis in travellers, Lancet Infect. Dis. 6 (6) (2006) 342–349.
- S.D. Lawn, J. Whetham, P.L. Chiodini, J. Kanagalilingam, J. Watson, R.H. Behrens, D.N. Lockwood, New world mucosal and cutaneous leishmaniasis: an emerging health problem among British travellers, QJM 97 (12) (2004) 781–788.
- D. Campbell-Lendrum, J.P. Dujardin, E. Martinez, M.D. Feliciangeli, J.E. Perez, L.N. Silans, P. Desjeux, Domestic and peridomestic transmission of American cutaneous leishmaniasis: changing epidemiological patterns present new control opportunities, Mem. Inst. Oswaldo Cruz 96 (2) (2001) 159–162.
- J.A. Patz, T.K. Graczyk, N. Geller, A.Y. Vittor, Effects of environmental change on emerging parasitic diseases, Int. J. Parasitol. 30 (12–13) (2000) 1395–1405.
- P. Desjeux, Leishmaniasis: current situation and new perspectives, Comp. Immunol. Microbiol. Infect. Dis. 27 (5) (2004) 305–318.
- J. Blum, P. Desjeux, E. Schwartz, B. Beck, C. Hatz, Treatment of cutaneous leishmaniasis among travellers, J. Antimicrob. Chemother. 53 (2) (2004) 158–166.
- R.D. Pearson, S.M.B. Jeronimo, A.Q. Sousa, in: S.H. Gillespie, R. D. P. (Org.) (Eds.), Principles and Practice of Clinical Parasitology, Vol. 1, John Wiley & Sons, Chichester, 2001, pp. 287–313.
- L. Sanchez-Saldana, Leishmaniasis, Dermatol. Peru 14 (2) (2004) 82–98.
- J. Ampuero Vela, Leishmaniasis, Ministerio de Salud, Lima, Peru, 2000.
- F. Modabber, P.A. Buffet, E. Torreele, G. Milon, S.L. Croft, Consultative meeting to develop a strategy for treatment of cutaneous leishmaniasis. Institute Pasteur, Paris. 13–15 June, 2006, Kinetoplastid Biol. Dis. 6 (2007) 3.
- P. Minodier, P. Parola, Cutaneous leishmaniasis treatment, Travel Med. Infect. Dis. 5 (3) (2007) 150–158.
- D. Vardy, Y. Barenholz, N. Naftoliev, S. Klaus, L. Gilead, S. Frankenburg, Efficacious topical treatment for human cutaneous leishmaniasis with ethanolic lipid amphotericin B, Trans. R. Soc. Trop. Med. Hyg. 95 (2) (2001) 184–186.
- A. Zvulunov, E. Cagnano, S. Frankenburg, Y. Barenholz, D. Vardy, Topical treatment of persistent cutaneous leishmaniasis with ethanolic lipid amphotericin B, Pediatr. Infect. Dis. J. 22 (6) (2003) 567–569.
- T. Hasan, B. Ortel, N. Solban, B. Pogue, in: B.R. Kufe DW, W.N. Hait, W.K. Hong, R. Pollock, R.R. Weichselbaum, H.J. Gansler T, E. Frei III (Eds.), Cancer Medicine, BC Decker Inc., Hamilton, Ontario, Canada, 2006, pp. 537–548.
- Y. Nitzan, H.M. Wexler, S.M. Finegold, Inactivation of anaerobic bacteria by various photosensitized porphyrins or by hemin, Curr. Microbiol. 29 (3) (1994) 125–131.
- P.G. Calzavara-Pinton, M. Venturini, R. Sala, A comprehensive overview of photodynamic therapy in the treatment of superficial fungal infections of the skin, J. Photochem. Photobiol. B 78 (1) (2005) 1–6.
- S. Sohl, F. Kauer, U. Paasch, J.C. Simon, Photodynamic treatment of cutaneous leishmaniasis, J. Dtsch Dermatol. Ges. 5 (2) (2007) 128–130.
- K. Pizinger, P. Cetkovska, D. Kacerovska, M. Kumpova, Successful treatment of cutaneous leishmaniasis by photodynamic therapy and cryotherapy, Eur. J. Dermatol. 19 (2) (2009) 172–173.
- E.M. van der Snoek, D.J. Robinson, J.J. van Hellemond, H.A. Neumann, A review of photodynamic therapy in cutaneous leishmaniasis, J. Eur. Acad. Dermatol. Venereol. 22 (8) (2008) 918–922.
- N.I.H. NIH Clinical Trials ID: NCT00840359, Study of the Efficacy of Daylight Activated Photodynamic Therapy in the Treatment of Cutaneous Leishmaniasis, Hadassah Medical Organization, vol. 2009, 2009.
- J. Montanari, A.P. Perez, F. Di Salvo, V. Diz, R. Barnadas, L. Dicelio, F. Doctorovich, M.J. Morilla, E.L. Romero, Photodynamic ultradeformable liposomes: design and characterization, Int. J. Pharm. 330 (1–2) (2007) 183–194.
- C.J.F. Bötcher, C.M. Van Gent, C. Pries, A rapid and sensitive submicro phosphorus determination, Anal. Chim. Acta 24 (1961) 203–204.
- C. Korzeniewski, D.M. Callewaert, An enzyme-release assay for natural cytotoxicity, J. Immunol. Meth. 64 (3) (1983) 313–320.
- F. Tietze, Enzymic method for quantitative determination of nanogram amounts of total and oxidized glutathione: applications to mammalian blood and other tissues, Anal. Biochem. 27 (3) (1969) 502–522.
- B.C. Walton, J.J. Shaw, R. Lainson, Observations on the *in vitro* cultivation of Leishmania braziliensis, J. Parasitol. 63 (6) (1977) 1118–1119.
- S.M. Harrison, B.W. Barry, P.H. Dugard, Effects of freezing on human skin permeability, J. Pharm. Pharmacol. 36 (4) (1984) 261–262.
- U. Schaefer, H. Loth, An *ex vivo* model for the study of drug penetration into human skin, Pharm. Res. 13 (1996) 66.
- D.W. Fry, J.C. White, I.D. Goldman, Rapid separation of low molecular weight solutes from liposomes without dilution, Anal. Biochem. 90 (2) (1978) 809–815.
- H. Wagner, K.H. Kostka, C.M. Lehr, U.F. Schaefer, Drug distribution in human skin using two different *in vitro* test systems: comparison with *in vivo* data, Pharm. Res. 17 (12) (2000) 1475–1481.



- 743 [36] F.L. Primo, M.M.A. Rodrigues, A.R. Simioni, M.V.L.B. Bentley, P.C. Morais, A.C.  
744 Tedesco, In vitro studies of cutaneous retention of magnetic nanoemulsion loaded  
745 with zinc phthalocyanine for synergic use in skin cancer treatment, *J. Magn. Magn.*  
746 *Mater.* 320 (2008) e211–e214.
- 747 [37] K.A. Mullin, B.J. Foth, S.C. Ilgoutz, J.M. Callaghan, J.L. Zawadzki, G.I. McFadden, M.J.  
748 McConville, Regulated degradation of an endoplasmic reticulum membrane  
749 protein in a tubular lysosome in *Leishmania mexicana*, *Mol. Biol. Cell* 12 (8)  
750 (2001) 2364–2377.
- 751 [38] G. Cevc, A. Schatzlein, H. Richardsen, Ultra-deformable lipid vesicles can penetrate  
752 the skin and other semi-permeable barriers unfragmented. Evidence from double  
753 label CLSM experiments and direct size measurements, *Biochim. Biophys. Acta*  
754 1564 (1) (2002) 21–30.
- 755 [39] P.L. Honeywell-Nguyen, H.W. Wouter Groenink, A.M. de Graaff, J.A. Bouwstra, The  
756 in vivo transport of elastic vesicles into human skin: effects of occlusion, volume  
757 and duration of application, *J. Control. Release* 90 (2) (2003) 243–255.
- 758 [40] P.L. Honeywell-Nguyen, G.S. Gooris, J.A. Bouwstra, Quantitative assessment of the  
759 transport of elastic and rigid vesicle components and a model drug from these  
760 vesicle formulations into human skin in vivo, *J. Invest. Dermatol.* 123 (5) (2004)  
761 902–910.
- 762 [41] A. Henning, U.F. Schaefer, D. Neumann, Potential pitfalls in skin permeation  
763 experiments: influence of experimental factors and subsequent data evaluation,  
764 *Eur. J. Pharm. Biopharm.* 72 (2) (2009) 324–331.
- 765 [42] J.-C. Tsai, M.J. Cappel, N.D. Weiner, G.L. Flynn, J.J. Ferry, Solvent effects on the  
766 harvesting of stratum corneum from hairless mouse skin through adhesive tape  
767 stripping in vitro, *Int. J. Pharm.* 68 (1–3) (1991) 127–133.
- 768 [43] B.A. van den Bergh, J.A. Bouwstra, H.E. Junginger, P.W. Wertz, Elasticity of vesicles  
769 affects hairless mouse skin structure and permeability, *J. Control. Release* 62 (3)  
770 (1999) 367–379.
- 771 [44] P.L. Honeywell-Nguyen, A.M. de Graaff, H.W. Groenink, J.A. Bouwstra, The in vivo  
772 and in vitro interactions of elastic and rigid vesicles with human skin, *Biochim.*  
773 *Biophys. Acta* 1573 (2) (2002) 130–140.
- 774 [45] K.A. Holbrook, G.F. Odland, Regional differences in the thickness (cell layers) of  
775 the human stratum corneum: an ultrastructural analysis, *J. Invest. Dermatol.* 62  
776 (4) (1974) 415–422.
- 777 [46] G. Cevc, G. Blume, Lipid vesicles penetrate into intact skin owing to the  
778 transdermal osmotic gradients and hydration force, *Biochim. Biophys. Acta*  
779 1104 (1) (1992) 226–232.
- 780 [47] J.P. Ryman-Rasmussen, J.E. Riviere, N.A. Monteiro-Riviere, Penetration of intact  
781 skin by quantum dots with diverse physicochemical properties, *Toxicol. Sci.* 91  
782 (1) (2006) 159–165.
- 783 [48] O.E. Akilov, S. Kosaka, K. O'Riordan, T. Hasan, Parasitocidal effect of delta-  
784 aminolevulinic acid-based photodynamic therapy for cutaneous leishmaniasis is  
785 indirect and mediated through the killing of the host cells, *Exp. Dermatol.* 16 (8)  
786 (2007) 651–660.
- 787 [49] C.D. Enk, C. Fritsch, F. Jonas, A. Nasereddin, A. Ingber, C.L. Jaffe, T. Ruzicka,  
788 Treatment of cutaneous leishmaniasis with photodynamic therapy, *Arch.*  
789 *Dermatol.* 139 (4) (2003) 432–434.
- 790 [50] K. Gardlo, S. Hanneken, T. Ruzicka, N.J. Neumann, Photodynamic therapy of  
791 cutaneous leishmaniasis. A promising new therapeutic modality, *Hautarzt* 55 (4)  
792 (2004) 381–383.
- 793 [51] K. Gardlo, Z. Horska, C.D. Enk, L. Rauch, M. Megahed, T. Ruzicka, C. Fritsch, 793  
794 Treatment of cutaneous leishmaniasis by photodynamic therapy, *J. Am. Acad.*  
795 *Dermatol.* 48 (6) (2003) 893–896.
- 796 [52] A. Asilian, M. Davami, Comparison between the efficacy of photodynamic therapy  
797 and topical paromomycin in the treatment of Old World cutaneous leishmaniasis:  
798 a placebo-controlled, randomized clinical trial, *Clin. Exp. Dermatol.* 31 (5) (2006)  
799 634–637.
- 800 [53] O.E. Akilov, S. Kosaka, K. O'Riordan, T. Hasan, Photodynamic therapy for cutaneous  
801 leishmaniasis: the effectiveness of topical phenothiaziniums in parasite eradica-  
802 tion and Th1 immune response stimulation, *Photochem. Photobiol. Sci.* 6 (10)  
803 (2007) 1067–1075.
- 804 [54] P. Escobar, I.P. Hernandez, C.M. Rueda, F. Martinez, E. Paez, Photodynamic activity  
805 of aluminium (III) and zinc (II) phthalocyanines in *Leishmania promastigotes*,  
806 *Biomedical* 26 (Suppl 1) (2006) 49–56.
- 807 [55] S. Dutta, D. Ray, B.K. Kolli, K.P. Chang, Photodynamic sensitization of *Leishmania*  
808 *amazonensis* in both extracellular and intracellular stages with aluminum  
809 phthalocyanine chloride for photolysis in vitro, *Antimicrob. Agents Chemother.*  
810 49 (11) (2005) 4474–4484.
- 811 [56] J. Moan, K. Berg, The photodegradation of porphyrins in cells can be used to  
812 estimate the lifetime of singlet oxygen, *Photochem. Photobiol.* 53 (4) (2001)  
813 549–553.
- 814 [57] A.P. Castano, T. Demidova, M.R. Hamblin, Mechanisms in photodynamic therapy:  
815 part one—photosensitizers, photochemistry and cellular localization, *Photodiagn.*  
816 *Photodyn. Ther.* 1 (4) (2004) 279–293.
- 817 [58] C.A. Robertson, D.H. Evans, H. Abrahamse, Photodynamic therapy (PDT): a short  
818 review on cellular mechanisms and cancer research applications for PDT, *J.*  
819 *Photochem. Photobiol. B* 96 (1) (2009) 1–8.
- 820 [59] A. Ketabchi, A. MacRobert, P.M. Speight, J.H. Bennett, Induction of apoptotic cell  
821 death by photodynamic therapy in human keratinocytes, *Arch. Oral Biol.* 43 (2)  
822 (1998) 143–149.
- 823 [60] S. Coppola, L. Ghibelli, GSH extrusion and the mitochondrial pathway of apoptotic  
824 signalling, *Biochem. Soc. Trans.* 28 (2) (2000) 56–61.
- 825 [61] R.M. Steinman, I.S. Mellman, W.A. Muller, Z.A. Cohn, Endocytosis and the recycling  
826 of plasma membrane, *J. Cell Biol.* 96 (1) (1983) 1–27.
- 827 [62] A. Papagiannaros, C. Bories, C. Demetzos, P.M. Loiseau, Antileishmanial and  
828 trypanocidal activities of new miltefosine liposomal formulations, *Biomed.*  
829 *Pharmacother.* 59 (10) (2005) 545–550.
- 830 [63] P. Overath, Y.D. Stierhof, M. Wiese, Endocytosis and secretion in trypanosomatid  
831 parasites – Tumultuous traffic in a pocket, *Trends Cell Biol.* 7 (1) (1997) 27–33.
- 832 [64] S.M. Landfear, M. Ignatushchenko, The flagellum and flagellar pocket of  
833 trypanosomatids, *Mol. Biochem. Parasitol.* 115 (1) (2001) 1–17.
- 834 [65] G. Cevc, in: Lipowsky, Sachman (Eds.), *Handbook of Biological Physics*, Vol. I,  
835 Elsevier Science BV, Amsterdam, 1995, pp. 465–489.
- 836 [66] P.L. Honeywell-Nguyen, J.A. Bouwstra, Vesicles as a tool for transdermal and  
837 dermal delivery, *Drug Discov. Today: Technol.* 2 (1) (2005) 67–74.
- 838 [67] J.A. Cowen, R.E. Imhof, P. Xiao, Opto-thermal measurement of stratum corneum  
839 renewal time, *Anal. Sci.* 17 (2001) s353–s356.
- 840 [68] J.P. Ryman-Rasmussen, J.E. Riviere, N.A. Monteiro-Riviere, Variables influencing  
841 interactions of untargeted quantum dot nanoparticles with skin cells and  
842 identification of biochemical modulators, *Nano Lett.* 7 (5) (2007) 1344–1348.